Using the SSMini pressuremeter for compaction quality control

Utilisation du pressiomètre SSMini pour le contrôle de la qualité du compactage

Brhane Weldeanenya Ygzaw[1#], *Paul John Cosentino*[1], and *Anuar Akchurin*[1], *Thaddeus J. Misilo*[2]

[1]*Florida Institute of Technology, Civil Engineering and Construction Management, Melbourne, Florida, USA*
[2]*Florida Institute of Technology, Information Technology, Melbourne, Florida, USA*

[#]*Corresponding author: bygzaw2022@my.fit.edu*

ABSTRACT

Nuclear density gauge (NDG) testing has been the standard for construction quality control (QC) for over six decades, despite its inability to assess soil strength and cumbersome logistics due to radiation. Recognizing these limitations, a fully automated small diameter pressuremeter (SSMini PMT) has been developed to measure soil strength and stiffness in under a minute. The device generates stress-strain data correlating with established testing methods, including a lightweight deflectometer, Klegg impact, dynamic cone, and nuclear density testing. With over 400 tests in sand and clay completed, the SSMini offers varying lengths (6 to 12 inches) of probes that fit NDG drive pinholes for seamless integration. This novel approach introduces a moisture-density-soil stiffness framework, enabling contractors to use targeted moisture contents alongside SSMini elastic modulus data to determine fill acceptability on-site. By directly measuring water content and modulus, this method eliminates the need for nuclear density testing, relying instead on the Proctor density for initial calibration. The SSMini PMT promises a safer, faster, and more precise QC process, marking a significant advancement in geotechnical engineering.

RESUME

Les tests de jauge de densité nucléaire (NDG) sont la norme pour le contrôle de la qualité de la construction (CQ) depuis plus de six décennies, malgré son incapacité à évaluer la résistance du sol et la logistique fastidieuse due aux radiations. Reconnaissant ces limites, un pressiomètre de petit diamètre entièrement automatisé (SSMini PMT) a été développé pour mesurer la résistance et la rigidité du sol en moins d'une minute. L'appareil génère des données de contrainte-déformation qui sont en corrélation avec les méthodes de test établies, notamment un déflectomètre léger, un impact Klegg, un cône dynamique et des tests de densité nucléaire. Avec plus de 400 tests réalisés dans le sable et l'argile, le SSMini propose différentes longueurs (6 à 12 pouces) de sondes qui s'adaptent aux trous d'entraînement NDG pour une intégration transparente. Cette nouvelle approche introduit un cadre de rigidité du sol en termes d'humidité-densité, permettant aux entrepreneurs d'utiliser des teneurs en humidité ciblées ainsi que des données de module d'élasticité SSMini pour déterminer l'acceptabilité du remblai sur site. En mesurant directement la teneur en eau et le module, cette méthode élimine complètement le besoin de tests de densité nucléaire, s'appuyant plutôt sur la densité Proctor pour l'étalonnage initial. Le SSMini PMT promet un processus de contrôle qualité plus sûr, plus rapide et plus précis, marquant une avancée significative dans l'ingénierie géotechnique.

Keywords: SSMini PMT; NDG; compaction; SSMini elastic modulus; degree of saturation

1. Introduction

1.1. Compaction quality control overview

For over six decades, the construction quality control (QC) industry has used nuclear density testing data to determine whether fill is acceptable. However, density is an index property, and the radiation associated with nuclear density gauge (NDG) testing produces serious logistics concerns. The Missouri Department of Transportation (MoDOT) reduced the amount of compaction QC using NDG and plans to stop using this machine completely (McLain and Gransberg 2017). Similarly, others, like the Indiana Department of Transportation, use a Lightweight Deflectometer (LWD) for compaction QC.

Density and water content-based compaction cannot consistently relate to layer stiffness and strength-dependent mechanistic-empirical approach (Cosentino 2024). Soil stiffness gauges, lightweight deflectometers, Klegg impact hammers, and dynamic cone penetrometers have all been suggested as alternatives to the NDG test process (Team 2007; Nazzal 2014; Fathi et al. 2020). No universal standard governs the various rollers and measuring the water content (Team 2007; Nazzal 2014; Fathi et al. 2020).

Several researchers (Heitor, Indraratna, and Rujikiatkamjorn 2016; Latimer, Airey, and Tatsuoka 2023) use nondestructive bender element triaxial type

tests to estimate small-strain shear stiffness, G_0, and propose an extensive compaction control framework governed by stiffness, degree of saturation, and compaction energy level (CEL). Developing the acceptable zone of compaction, considering the effect of these compaction-controlling parameters, is helpful; however, the in-situ evaluation of G_0 during the actual compaction is extremely complex.

1.2. Pressuremeter overview

In 1954, Menard, a young intern student who was checking the compaction of an airport earthwork in France, invented the first Tricell pressuremeter (PMT) with the hope of using it for compaction QC. However, his original goal remained largely unmet due to practical limitations. Typical compacted fill layers are relatively thin, usually between 20 and 30 cm, which is insufficient to accommodate the standard pressuremeter probe, whose dimensions and influence zone exceed the thickness of a single lift. As a result, the conventional PMT could not be effectively used to assess individual layers of compacted fill. In 2016, Cosentino and Misilo (Cosentino et al. 2018; Cosentino and Misilo 2023; Cosentino and Misilo 2021) developed what was originally called the small-diameter PMT to fit in the pinhole used during NDG testing. This PMT was tested alongside NDG, lightweight deflectometers (LWD), Klegg impact hammers, and dynamic cone penetrometers. Excellent correlations were produced between this SSMini elastic modulus ($E_{0\text{-SSMini}}$) and limit pressure (pL), which led to funding through the National Cooperative Research Program (NCHRP) Innovations Deserving Exploratory Analysis (IDEA) funding through project number 244. During this work, the small-diameter PMT was renamed to the SSMini PMT, as the entire set of equipment was developed for market use and production to yield strength (pL) and stiffness in less than a minute (Cosentino et al. 2018)SSMini 6-, 8-, 10-, and 12-inch long ¾-inch diameter probes fit in the same pinhole made during NDG testing, enabling testing of layers from 6 to 12 inches.

2. Methods

2.1. SSMini PMT development and working principle

The SSMini PMT equipment was improved from a research-level device to a market-ready device under NCHRP IDEA 244. Fig. 1 shows the major components of the fully automated SSMini PMT.

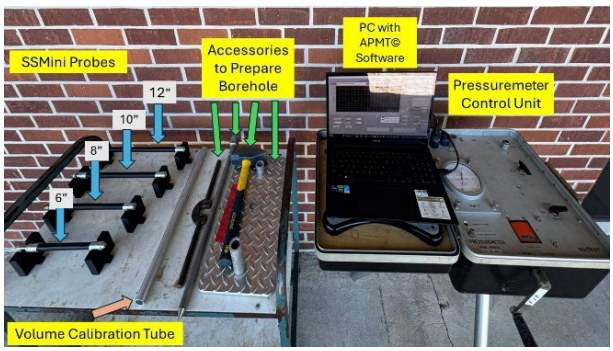

Fig. 1 SSMini PMT Components

SSMini PMT tests are completed by injecting water into the rubber balloon, which applies pressure to the borehole wall. The equipment includes three data acquisition and processing software programs. The testing procedures were developed during the original Florida Department of Transportation (FDOT) funded research under contract BDV28 977-04 Development and Testing of the Miniaturized Pavement Pressuremeter for Use in Unbound Pavement Layers (Cosentino et al. 2018). In addition to the hand-operated incremental type, a motor-controlled, fully automated SSMini PMT that works incrementally and continuously has been developed (Cosentino 2024).

The hole for the SSMini PMT is usually prepared using the metal drive pin used for NDG testing. It may also be prepared by drilling the hole using a long bit and the NDG template. To evaluate the SSMini results, SP sands were compacted at optimum moisture. Using a drill bit and the NDG drive pin 36, SSMini tests were conducted at the FIT Applied Research Lab, producing E0-SSMini and pL results within 10 percent.

The SSMini PMT probe was inserted either using a drive pin or into pre-drilled holes to evaluate the effects of insertion on measurement repeatability. The drive pin method may somehow mimic an unload-reload cycle by pushing the soil aside during insertion (loading) and allowing it to relax (unloading) before reloading during pressurization. Interestingly, results show that variability remains low across both methods: the coefficient of variation (COV) for the initial modulus E_0 ranged from 14% to 18%, and the limit pressure pL ranged from 16% to 20%, indicating acceptable repeatability for in-situ testing (Briaud 2023). Further control testing under incremental and continuous loading yielded even lower COVs, typically between 6% and 10%, demonstrating the tool's consistent performance. Additionally, testing with augered holes, where less lateral or downward disturbance occurs compared to drive pin insertion, resulted in similarly low variability (within 10%). This consistency across insertion methods, both of which are part of the NDG standard, suggests that the influence of insertion on measurement results is minimal.

2.2. Interpretation, processing, and correlation of SSMini PMT test results

A sample SSMini PMT test is shown in Fig. 2, where $E_{0\text{-SSMini}}$ is computed from the linear soil response portion of the stress versus volume curve, as shown in Fig. 2 (a), and pL, defined as the soil strength when the volume of

a deformed borehole or injected water is doubled, is estimated from the stress versus volumetric strain curve at a volumetric strain of 1 or 100%, as shown in Fig. 2 (b).

$$E_0 = 2*(1+\upsilon)*\frac{(P_2 - P_1)}{(\Delta V_1 - \Delta V_2)}*(V_0 + 0.5*(\Delta V_1 + \Delta V_2)) \quad (1)$$

where υ is Poisson's ratio, ΔP_1, ΔP_2, ΔV_1, and ΔV_2 are the pressures and volumes, Fig. 2 (a), and V_0 is the volume of the uninflated probe.

A summary of the original SSMini research is shown in Table 1. Correlations between SSMini $E_{0\text{-SSMini}}$ and pL

The SSMini PMT modulus is computed from the linear soil response portion of the stress-volume curve using Eq. (1):

and two LWD models indicate that both LWD moduli compare well to SSMini elastic moduli. This research also showed a significant amount of scatter between direct comparisons from LWD data (Cosentino and Misilo 2023).

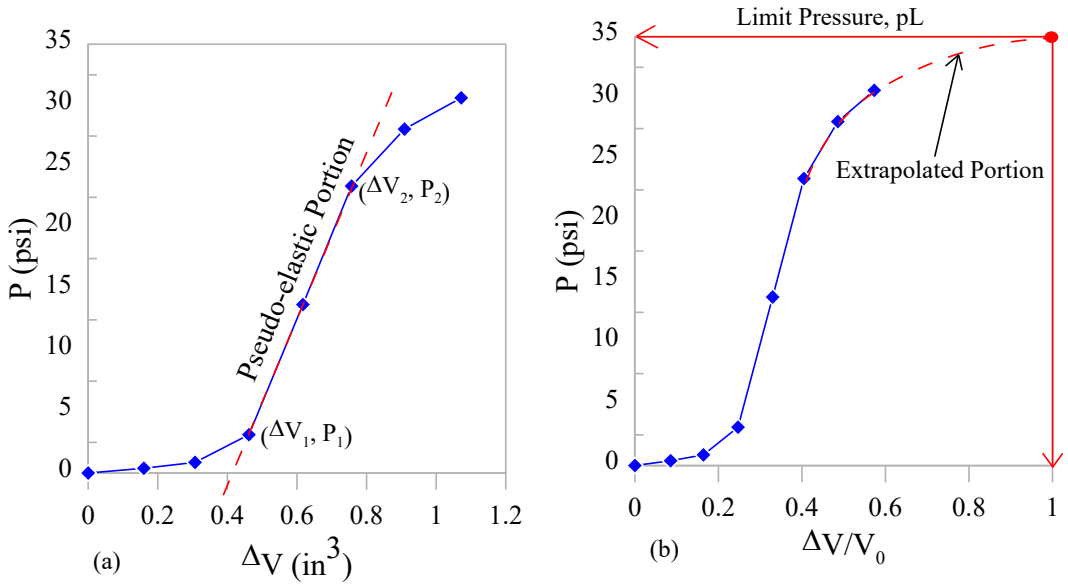

Fig. 2 Sample SSMini PMT test results

Table 1. Correlation between SSMini PMT parameters and LWD moduli

Test Type	Zorn LWD			Dynatest LWD		
	No of Tests	Correlation	R^2	No of Tests	Correlation	R^2
SDPMT-6" Incremental	35	$E_{0,\,Zorn}=1426\,(E_{0\text{-SSMini}})^{0.39}$	0.82	33	$E_{0,\,Dynatest}=3936\,(E_{0\text{-SSMini}})^{0.47}$	0.75
SDPMT-6" Continuous	33	$E_{0,\,Zorn}=75.77\,(E_{0\text{-SSMini}})^{0.67}$	0.87	31	$E_{0,\,Dynatest}=43.55\,(E_{0\text{-SSMini}})^{0.9}$	0.82
SDPMT-12" Incremental	46	$E_{0,\,Zorn}=148.3\,(E_{0\text{-SSMini}})^{0.64}$	0.86	44	$E_{0,\,Dynatest}=81.48\,(E_{0\text{-SSMini}})^{0.88}$	0.77
SDPMT-12" Continuous	39	$E_{0,\,Zorn}=230.8\,(E_{0\text{-SSMini}})^{0.57}$	0.86	38	$E_{0,\,Dynatest}=120.7\,(E_{0\text{-SSMini}})^{0.8}$	0.85
SDPMT-6" Incremental	35	$E_{0,\,Zorn}=1540\,(pL)^{0.51}$	0.88	33	$E_{0,\,Dynatest}=2132\,(pL)^{0.69}$	0.86
SDPMT-6" Continuous	33	$E_{0,\,Zorn}=211.5\,(pL)^{0.81}$	0.88	31	$E_{0,\,Dynatest}=39.42\,(pL)^{1.27}$	0.83
SDPMT-12" Incremental	46	$E_{0,\,Zorn}=438.5\,(pL)^{0.72}$	0.86	44	$E_{0,\,Dynatest}=396.5\,(pL)^{0.97}$	0.77
SDPMT-12" Continuous	40	$E_{0,\,Zorn}=453.4\,(pL)^{0.71}$	0.88	38	$E_{0,\,Dynatest}=576.1\,(pL)^{0.91}$	0.74

2.3. NDG-SSMini PMT sequential testing

The SSMini PMT probe was developed to fit the commonly used thicknesses associated with a compaction lift, 12 inches (Cosentino et al. 2018). During this research, the SSMini PMT probe was immediately inserted into the pinhole after NDG testing; therefore, this testing procedure was termed sequential testing. All the data presented here are collected according to this sequential procedure.

Sequential tests were conducted at two indoor controlled testing pits and three outdoor sites on Florida's poorly graded (SP) fine sands and a group of clays (CL, SC, SW-SC-, GC, GW-GC) from a series of active

projects in Virginia's Piedmont clays. Tests were conducted at the FDOT State Materials Office (SMO) indoor pits, where SP sands from two quarry sites, one weak and another strong, were compacted at optimum moisture content and 90%, 95%, and 100% modified Proctor maximum dry density. The two 24-foot-long, 9-foot-wide, and 7-foot-deep pits are separated into three parts. Tests were also conducted at FDOT's outdoor test sites in Kingsley and Trenton, Florida, and an active construction site provided by ECS Tampa in Sarasota, Florida. The sequential tests conducted in Virginia are on various construction sites that are dominantly Piedmont clays.

Table 2 shows the classification of the soils, maximum dry density (MDD), optimum moisture content (OMC), specific gravity (Gs), and number of sequential tests conducted in each site.

Table 2. Sequential Tests Conducted in Piedmont Clays

USCS Classification	MDD (pcf)		OMC (%)		Average Gs	No of tests	Test Method
	Minimum	Maximum	Minimum	Maximum			
CL	106	128.7	10.3	17.4	2.61	33	Sequential Testing
GC	118.9	125.5	10.2	13.9	2.6	21	
SC	114.9	128.8	10.6	16.2	2.68	20	
SM	107.7	124.8	11	17.8	2.6	10	
SW-SC	130.6		11.6		2.6	3	
GW-GC	139.5		7.1		2.79	4	
ML	107.7		17.8		2.6	5	

The most significant advantage of the SSMini PMT test is that it immediately produces in situ strength and stiffness. The correlation between the strength and stiffness for this test is strong, which can also be used to check the quality of a test. Fig. 3 (a) shows the correlation between the SSMini elastic modulus and limit pressure from 201 sequential SSMini NDG tests collected from the sites listed above. The correlation coefficient of 14.5 for the $E_{0\text{-SSMini}}$ vs. pL is when mc data from all types of soils with different site conditions are plotted in one.

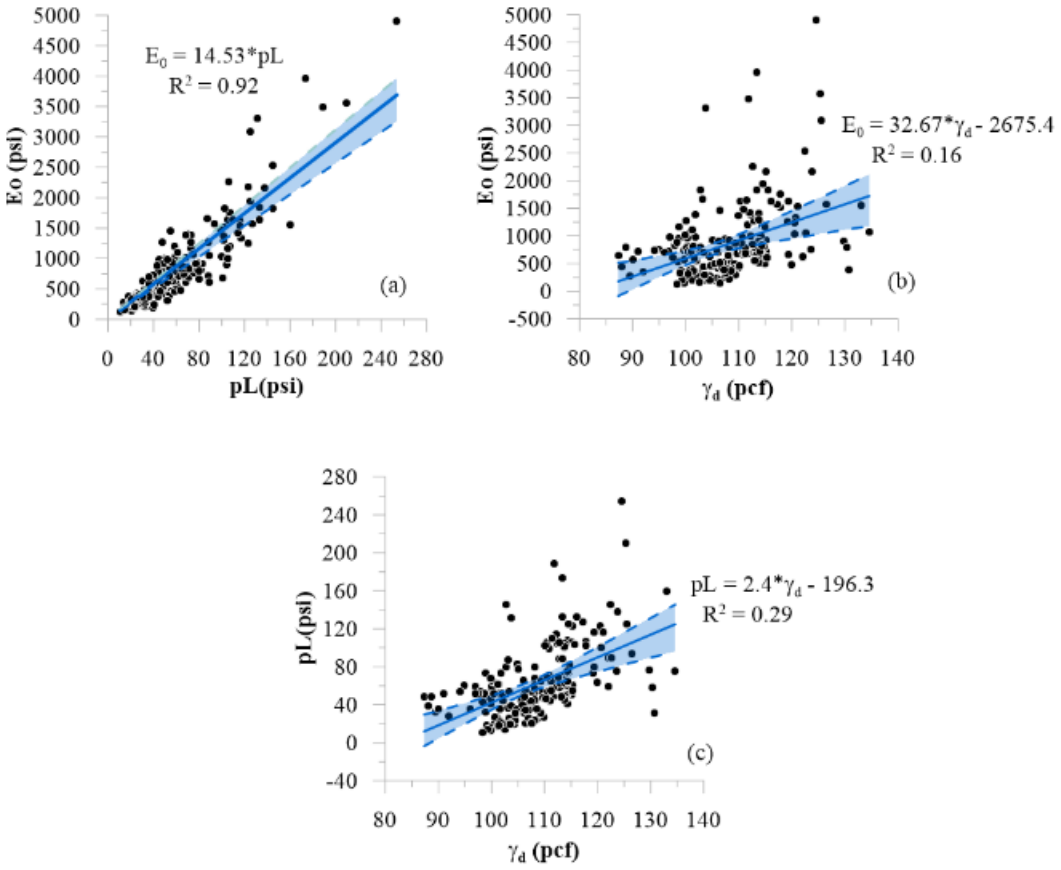

Fig. 3 Correlation between $E_{0\text{-SSMini}}$, pL, and γ_{dry} for the data from six sites

Fig. 3 (b) and (c) depict a poor correlation of dry density with initial modulus and limit pressure, respectively. Independent research also confirmed that there is no defined relation exists between the density and stiffness or modulus of a compacted fill. Concluding that compacted fill and dry density may or may not always guarantee a higher strength or stiffness (McLain and

Gransberg 2017; Heitor, Indraratna, and Rujikiatkamjorn 2016; Look 2022).

2.4. Parameters controlling the compaction process

Traditional soil compaction is dominantly based on the dry density of compacted soil. Every effort is made to attain the target density (γ_{dry}) max, the maximum dry density attained in the laboratory Proctor test. However, this density neither strongly correlates with the basic soil parameters used for the design nor is used directly in the design process. Moreover, density alone cannot control the compaction QC. It is worth investigating the parameters that play the main role in compaction. Test pits were prepared at FDOT-SMO to study what parameters control the compaction process and to propose a compaction QC framework accordingly.

The compaction process in the FDOT-SMO indoor pit was completed with care, and the results revealed imperative interaction at different stages of compaction. The test pits were prepared for two poorly graded sands; one was stronger from a test pit called Starvation Hill (SH), and the other was weaker from a test pit called Osteen (OST). compacted at 90%, 95%, and 100% modified Proctor.

The tests in the FDOT-SMO were not done immediately after compaction; therefore, the compacted soil was slightly dry during testing.

Fig. 4 shows the Proctor test results of SH and OST sands. The combination of OMC, maximum dry density ($\gamma_{dry\ max}$), and optimum degree of saturation are 10.6%, 114 pcf, and 62% for SH, 14%, 106.4 pcf, and 67% for OST. Tests for both pits showed that the moisture content and S_r indicated that all the results were dry of the optimum moisture content.

Considering the basic behavior of soils, a high matrix suction potential exists when it is dry, which decreases to about zero when it is close to 100 percent saturation. At a constant water content, if the compaction energy or the number of passes is increased, the dry density increases, and the degree of saturation increases.

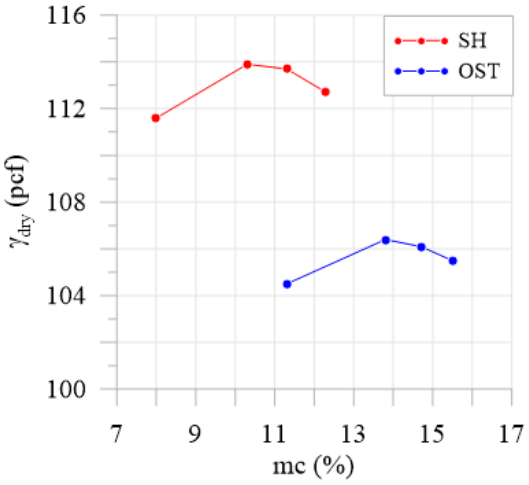

Fig. 4 Proctor test results from poorly graded SH and OST sands

However, both the suction potential and effective stress decrease, and hence SSMini elastic modulus decreases (Latimer, Airey, and Tatsuoka 2023; Tatsuoka and Miura 2019; Tatsuoka, Hashimoto, and Tateyama 2021). The test results from the different sites, especially data from FDOT-SMO, were checked to see if these basic behaviors could be observed. A positive correlation was observed between γ_{dry} and S_r, while $E_{0\text{-}SSMini}$ and S_r produced a negative correlation at two fixed moisture contents, as depicted in Fig. 5.

Keeping the dry density constant, Fig. 6, if the degree of saturation is increased, the SSMini elastic modulus decreases due to the decrease in matric suction and over-compaction. This indicates that S_r is one of the key parameters that control compaction. This was also confirmed by (Tatsuoka and Miura 2019) with more test data on similar soil types.

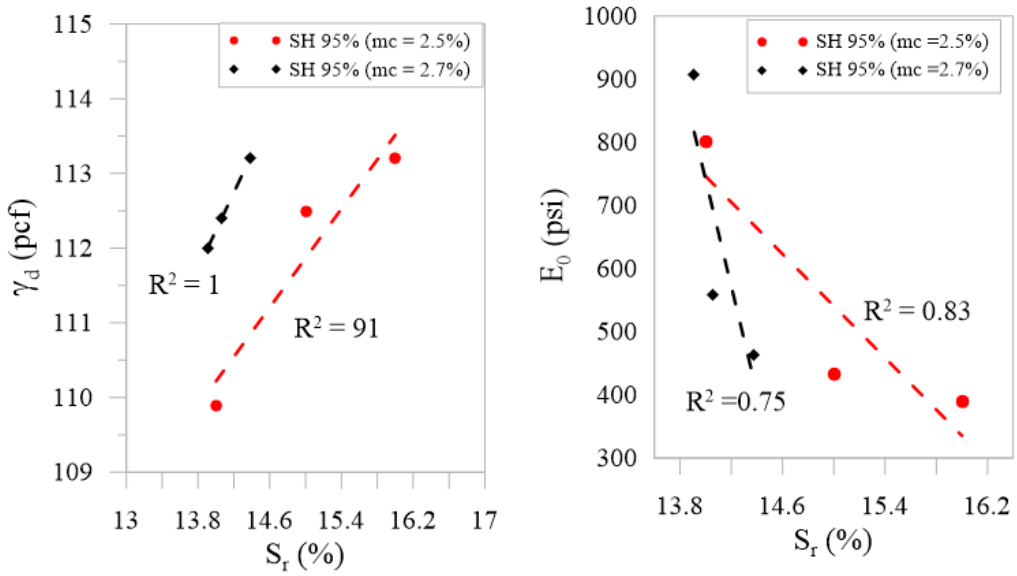

Fig. 5 Relationship of Sr with γ_{dry} and $E_{0\text{-}SSMini}$ at a fixed water content

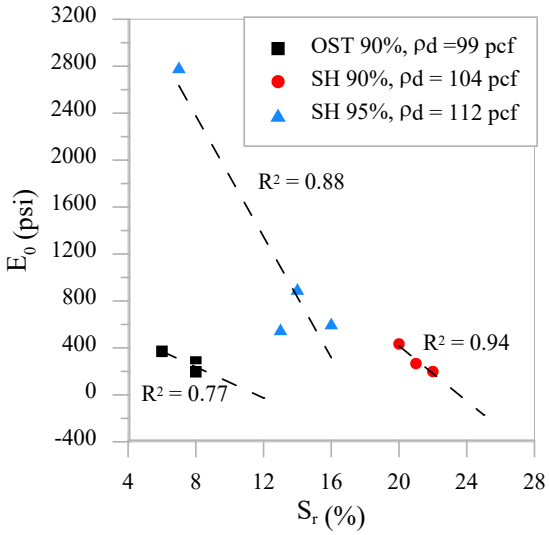

Fig. 6 Relationships between $E_{0\text{-}SSMini}$ and S_r for constant dry densities

On the other hand, keeping S_r constant, Fig. 7 shows $E_{0\text{-}SSMini}$ increases as γ_{dry} increases. Therefore, both S_r and γ_{dry} control compaction. Eq. (2) is an empirical relationship where a soil stiffness index (SSI) is expressed as a function of S_r and γ_{dry} (Tatsuoka, Hashimoto, and Tateyama 2021).

$$E_{0-SSMini} = E_{0-SSMini}(S_r) * \left(\frac{\gamma_d}{\gamma_w} - b\right)^c = a * \left(\frac{\gamma_d}{\gamma_w} - b\right)^c \quad (2)$$

Where $E_{0\text{-}SSMini}(S_r)$ is a coefficient and a function of S_r, this coefficient controls the effect of S_r on the compaction process. Depending on the results from the large-scale compaction data (Tatsuoka, Hashimoto, and Tateyama 2021), the parameters b and c can be taken as 0 and 9.5, respectively. Since the data collected at the FDOT-SMO is limited to the optimum dry side, there is not enough data to develop the complete "a" versus S_r curve. However, this data will fill the gap in the compaction behavior of compacted soil at lower S_r, which has not been covered so far.

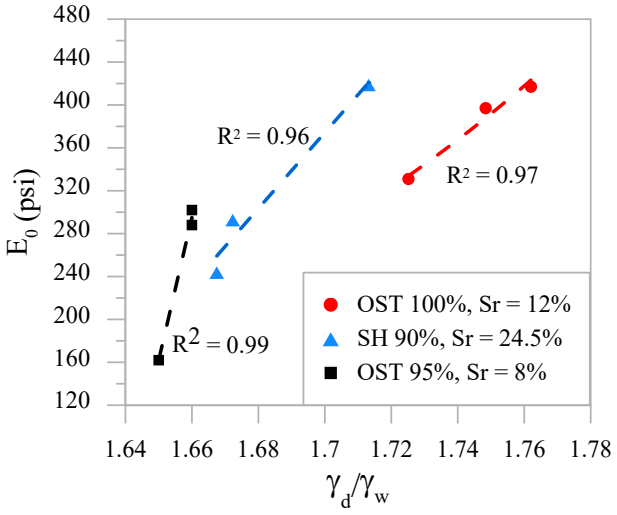

Fig. 7 Sample correlation between elastic modulus and dry density at constant degrees of saturation

Research studies based on compaction test data from sand and silty sands showed that a Boltzmann sigmoidal model relationship exists between G_0 and S_r, like the one shown in Fig. 8 (Latimer, Airey, and Tatsuoka 2023). Even though there are ranges of correlations between elastic modulus and small-strain shear modulus, G_0 in literature, $0.8*G_0$ (Robertson 2009) is considered here. Furthermore, $E_{0\text{-}SSMini}$ for SSMini PMT is approximately equal to $E*\alpha$, where α is a rheological factor that depends on the type of soil and consolidation history (Ménard and Rousseau 1962).

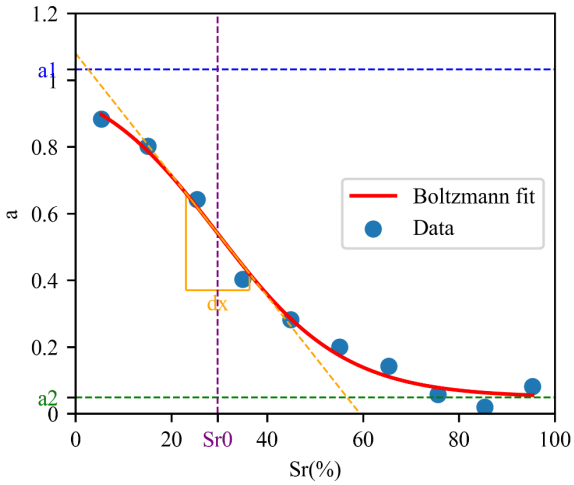

Fig. 8 Boltzmann sigmoidal model fitting between a and S_r adopted for $E_{0\text{-}SSMini}$

A Boltzmann fitting curve, Eq. (3), models this data well.

$$E_0(S_r) = \frac{(a_1 - a_2)}{1 + \exp\frac{(S_r - S_{r,0})}{dx}} + a_2 \quad (3)$$

Where a_1 is the upper asymptote value, a_2 is the lower asymptote value; Sr_0 is the inflection point (the Sr value at the midpoint of the transition), and S_r is computed easily using Eq. (4), and dx is the slope factor as indicated in Fig. 8.

$$S_r = \frac{mc * \gamma_d * G_s}{(\gamma_w * G_s - \gamma_d)} \quad (4)$$

In Eq. (4), mc and γ_d are the moisture content and dry density at any stage during compaction, G_s is the specific gravity of the soil, and γ_w is the density of water.

After substituting the values of each term into Eq. (*3*), the Boltzmann model for Fig. 8 will be as given in Eq. (5).

$$E_0(S_r) = \frac{(1.033 - 0.049)}{1 + \exp\frac{(S_r - 29.65)}{13.239}} + 0.049 \quad (5)$$

The complete empirical formula, including the parameters that control compaction, can be rewritten as Eq. (*6*), which reveals that the SSMini elastic modulus is a function of S_r and γ_{dry} for a given soil type.

$$E_{0-SSMini} = \left[\frac{(a_1 - a_2)}{1 + \exp^{\frac{(S_r - S_{r,0})}{dx}}} + a_2 \right] * \left(\frac{\gamma_d}{\gamma_w} \right)^c \qquad (6)$$

Using Eq.s (*4*) and (*6*), contour lines for S_r and $E_{0\text{-}SSMini}$ can be developed in the γ_d-mc plane. Referring to Fig. 9, the two points of the 98% degree of compaction are indicated, and S_r and $E_{0\text{-}SSMini}$ contours that pass through these points are shown. For the case provided in Fig. 9, $S_{r,\,min}$ = 57%, the minimum degree of saturation this specific soil needs to attain the required degree of compaction. On the contrary, S_r = 81% indicates the maximum degree of saturation needed to satisfy the required degree of compaction, 98% degree of compaction in this case. Moreover, the two SSMini elastic moduli at these points are also easily computed using Eq. (6).

There are essential points in Fig. 9 that are worth elaborating on. First, the contour spacing of the $E_{0\text{-}SSMini}$ lines is not uniform at different regions of the γ_d-mc plane. On the dry optimum side, a slight decrease in the degree of saturation results in a significant increase in $E_{0\text{-}SSMini}$. However, it is the opposite on the wet optimum side. Second, even though the $E_{0\text{-}SSMini}$ values are higher when the water content is lower, it does not guarantee that this is the safe zone to be considered during compaction. This variation will have vast consequences during the service life of the compacted fill when it gets wet, and a higher degree of saturation than during compaction is attained.

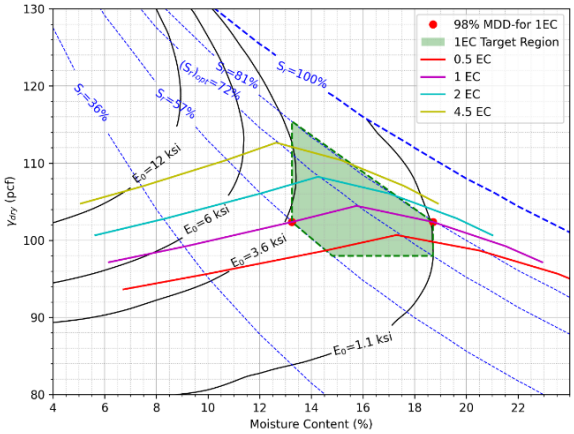

Fig. 9 Sample Compaction Target (Acceptable) Region

The minimum and maximum S_r and $E_{0\text{-}SSMini}$ threshold levels are shown in Fig. 9, along with compaction energy levels (CELs) based on standard Proctor, between ½ and 4.5 times the standard energy level. Based on 98 percent of the maximum dry density, the field compaction water content target region is related to two points between 57 and 81 percent saturation. The field CEL should also be known as part of the compaction controlling variables. Referring to the same figure, the upper and lower boundaries of the target curve are controlled by the actual CEL (i.e., 98 percent curve). This data shows that the field moisture content should range from about 13 to just below 19 percent, a reasonable range for compaction QC.

Eq. (7**)** is an empirical relationship between the (γ_d)max for the 1 EC and other EC's at different CEL (Tatsuoka 2015).

$$\left[(\gamma_d)_{\max} \right]_{field} = \left[(\gamma_d)_{\max} \right]_{1EC} * \left[1 + c * \log\left(\frac{CEL}{EC} \right) \right] \qquad (7)$$

Where c is a coefficient, data collected from a large number of samples is recommended to be 0.12.

After developing the acceptable region, the field compaction is controlled by aiming at the target CEL and keeping the water content around OMC. Then, the SSMini elastic modulus is checked to see if it is within the acceptable region. Moreover, apart from compaction QC, predicted settlement for a known load and size of footing can be computed**.** Fig. 10 shows the contour of settlements for the selected soil in reference to the acceptable region.

Fig. 10 provides a chance to decide whether to reduce the load so that the maximum calculated settlement in the Target region is less than or equal to the tolerable settlement limit, usually 1 inch, or to increase the minimum $E_{0\text{-}SSMini}$, which reduces the area of the acceptable region.

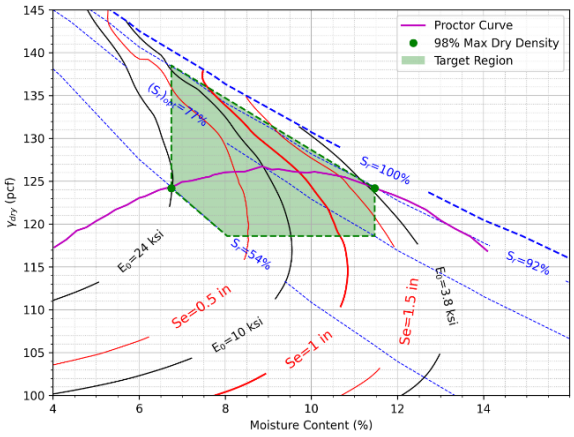

Fig. 10 Degree of Saturation, SSMini Elastic Moduli, and Settlement Contours within the Target Region

3. Conclusions

SSMini PMT testing from over 400 tests with NDG equipment produced reliable data.

The Boltzmann sigmoidal-based modeling using SSMini $E_{0\text{-}SSMini}$, degree of saturation, and moisture density produced a reasonable range of field moisture contents that contractors can follow.

The new $E_{0\text{-}SSMini}$-S_r-CEL-based compaction QC procedure is a promising method for combining moisture density with SSMini elastic moduli to determine compaction QC acceptability.

Acknowledgments

The authors acknowledge the support of the NCHRP IDEA Type 2 program, guided by Inam Jawed. Sincere thanks go to the Florida Department of Transportation, especially David Horhota, Ph.D., P.E., Travis Dalton Williams, Todd Britton, Bruce Swidarski, Mike Risher, Kelly Shislova, and Dino Jameson of the Gainesville State Materials Research Office, for providing numerous

test sites in Gainesville and Orlando. Thanks are also due to ECS, LLC, particularly the Tampa, Orlando, and Chantilly, Virginia offices, for supporting tests in sands and clays. Thanks to Karl A. Higgins III, Mehmetali Uzan, Antonio Giordano, and Scott M. Nelson for their contributions. Appreciation is expressed to Bansbach Easylift of North America Inc., led by Robert T. Rose and Esteban Contreras, for manufacturing the SSMini cylinder and control systems, and to Marcello Canitano of Brevard Precision, LLC, for producing the SSMini probes.

References

Cosentino, P. J., Thaddeus J. Misilo III, Alaa M. Shaban, and Jacob W. Janson. 2018. "Development and Testing of the Miniaturized Pavement Pressuremeter for Use in Unbound Pavement Layers." Florida Department of Transportation. https://rosap.ntl.bts.gov/view/dot/65674.

Cosentino, Paul J. 2024. "Development of a Compaction Quality Control Standard for the Small Diameter Pressuremeter." https://trid.trb.org/View/2452655.

Cosentino, Paul J., and Thaddeus J. Misilo Iii. 2021. "Comparing Engineering Properties of Small Diameter Pressuremeter Tests to Clegg Impact Hammer Tests in Cemented Coquina Base and Sandy Subgrades." *Geotechnical Testing Journal* 44 (5): 1261–78. https://doi.org/10.1520/GTJ20190421.

Cosentino, Paul J., and Thaddeus J. Misilo. 2023. "Comparing Engineering Properties from Small Diameter Pressuremeter Tests to Nuclear Density Unit Weights and Lightweight Deflectometer Stiffnesses in Cemented Coquina Base and Sandy Subgrades." *Journal of Testing and Evaluation* 51 (2): 20210336. https://doi.org/10.1520/JTE20210336.

Cosentino, Paul John. 2024. "Development of a Compaction Quality Control Standard for the Small Diameter Pressuremeter." NCHRP IDEA Program Final Report IDEA Project NCHRP-244. FHWA. https://www.dropbox.com/scl/fi/cup7w8gmj20b8hjjrq53y/NCHRP-IDEA-244-Final-Report-Cosentino-FIT-June-27-2024.pdf?dl=0&rlkey=8rwtsj7a1mg5vwbq3amxus1nf&st=zmhor5j5.

Fathi, Aria, Cesar Tirado, Sergio Rocha, Mehran Mazari, and Soheil Nazarian. 2020. "Incorporating Calibrated Numerical Models in Estimating Moduli of Compacted Geomaterials from Integrated Intelligent Compaction Measurements and Laboratory Testing." *Transportation Research Record: Journal of the Transportation Research Board* 2674 (4): 75–88. https://doi.org/10.1177/0361198120912743.

Heitor, Ana, B. Indraratna, and Cholachat Rujikiatkamjorn. 2016. "Small Strain Behaviour of a Compacted Subgrade Soil." *Procedia Engineering* 143 (December):260–67. https://doi.org/10.1016/j.proeng.2016.06.033.

Latimer, R., D. Airey, and F. Tatsuoka. 2023. "Expected Stiffness Changes during Compaction in Laboratory and Field." *Transportation Geotechnics* 43:101136. https://www.sciencedirect.com/science/article/pii/S221439122300209X.

Look, Burt G. 2022. "An Earthworks Quality Assurance Methodology Which Avoids Unreliable Correlations." In *Advances in Transportation Geotechnics IV*, edited by Erol Tutumluer, Soheil Nazarian, Imad Al-Qadi, and Issam I.A. Qamhia, 166:179–92. Lecture Notes in Civil Engineering. Cham: Springer International Publishing. https://doi.org/10.1007/978-3-030-77238-3_14.

McLain, Kevin W., and Douglas D. Gransberg. 2017. "Contractor-Furnished Compaction Testing: Searching for Correlations between Potential Alternatives to the Nuclear Density Gauge in Missouri Highway Projects." *International Journal of Quality and Innovation* 3 (2/3/4): 91. https://doi.org/10.1504/IJQI.2017.090532.

Ménard, Louis, and J. Rousseau. 1962. "L'évaluation Des Tassements, Tendances Nouvelles." *Sols Soils* 1 (1): 13–29.

Nazzal, Munir. 2014. *Non-Nuclear Methods for Compaction Control of Unbound Materials*. Project 20-05, Topic 44-10. https://trid.trb.org/View/1302204.

Robertson, P. K. 2009. "Interpretation of Cone Penetration Tests — a Unified Approach." *Canadian Geotechnical Journal* 46 (11): 1337–55. https://doi.org/10.1139/T09-065.

Tatsuoka, Fumio. 2015. "Compaction Characteristics and Physical Properties of Compacted Soil Controlled by the Degree of Saturation." In *Geotechnical Synergy in Buenos Aires 2015*, 435–71. IOS Press. https://ebooks.iospress.nl/doi/10.3233/978-1-61499-599-9-435.

Tatsuoka, Fumio, Takeshi Hashimoto, and Kazuyoshi Tateyama. 2021. "Soil Stiffness as a Function of Dry Density and the Degree of Saturation for Compaction Control." *Soils and Foundations* 61 (4): 989–1002. https://www.sciencedirect.com/science/article/pii/S0038080621000871.

Tatsuoka, Fumio, and Toru Miura. 2019. "Compacted States and Physical Properties of Soil Controlled by the Degree of Saturation during Compaction." In *E3S Web of Conferences*, 92:18002. EDP Sciences. https://www.e3s-conferences.org/articles/e3sconf/abs/2019/18/e3sconf_isg2019_18002/e3sconf_isg2019_18002.html.

Team, E. C. T. 2007. "Soil-Stiffness Gauge for Soil Compaction Control." https://docs.lib.purdue.edu/ectfs/80/.

Briaud, Jean-Louis. 2023. *Geotechnical Engineering: Unsaturated and Saturated Soils*. John Wiley & Sons. https://books.google.com/books?hl=en&lr=&id=dgTLEAAAQBAJ&oi=fnd&pg=PA1&dq=%E2%80%A2%09Briaud,+J.-L.+(2013).+Geotechnical+Engineering:+Unsaturated+and+Saturated+Soils.+Wiley&ots=3ac2SHLMQx&sig=4J8J3evUk2q688ryon2sgs-ChS0.